Clinical Neurophysiology 124 (2013) 675–685

Contents lists available at SciVerse ScienceDirect

Clinical Neurophysiology

journal homepage: www.elsevier.com/locate/clinph

Mapping repetition suppression of the P50 evoked response to the human cerebral cortex

Nash N. Boutros [a,*,1], Klevest Gjini [a], Simon B. Eickhoff [b], Horst Urbach [c,2], Mark E. Pflieger [d]

[a] Wayne State University, School of Medicine, Department of Psychiatry and Behavioral Neurosciences, Detroit, MI, USA
[b] Institute for Neuroscience and Medicine (INM-2), Research Center Jülich, and Institute for Clinical Neuroscience and Medical Psychology, Heinrich-Heine University, Düsseldorf, Germany
[c] Neuro-Radiology Department, Bonn University Clinic, Bonn, Germany
[d] Source Signal Imaging, La Mesa, CA, USA

ARTICLE INFO

Article history:
Accepted 8 October 2012
Available online 4 November 2012

Keywords:
Habituation
P50
Repetition suppression
Sensory gating
Cingulate
Parietal lobe

HIGHLIGHTS

- We mapped the cortical regions contributing to repetition suppression (RS).
- Cingulate, parietal, as well as new frontal lobe regions were shown for the first time to be involved.
- Data highlights the complex system mediating RS in the human brain.

ABSTRACT

Objective: The cerebral network subserving repetition suppression (RS) of the P50 auditory evoked response as observed using paired-identical-stimulus (S1–S2) paradigms is not well-described.
Methods: We analyzed S1–S2 data from electrodes placed on the cortices of 64 epilepsy patients. We identified regions with maximal amplitude responses to S1 (i.e., stimulus registration), regions with maximal suppression of responses to S2 relative to S1 (i.e., RS), and regions with no or minimal RS 30–80 ms post stimulation.
Results: Several temporal, parietal and cingulate area regions were shown to have significant initial registration activity (i.e., strong P50 response to S1). Moreover, prefrontal, cingulate, and parietal lobe regions not previously proposed to be part of the P50 habituation neural circuitry were found to exhibit significant RS.
Conclusions: The data suggest that the neural network underlying the initial phases of the RS process may include regions not previously thought to be involved like the parietal and cingulate cortexes. In addition, a significant role for the frontal lobe in mediating this function is supported.
Significance: A number of regions of interest are identified through invasive recording that will allow further probing of the RS function using less invasive technology.

1. Introduction

The ability to suppress responses to incoming redundant sensory input (i.e., habituation) is a recognized characteristic of the central nervous system (CNS) (Venables, 1964; Eisenstein and Eisenstein, 2006). Habituation has been postulated as a protective function for the CNS, failure of which is proposed as a significant contributor to cognitive dysfunction or psychosis. The cerebral networks and processes, by which this function is mediated, however, are far from being well-described. Habituation in the CNS has been extensively studied utilizing Evoked Potential (EP) methodologies (Cromwell et al., 2008). In particular, the P50 and N100 auditory evoked responses (AERs) have been used to examine habituation using repetition suppression (RS) paradigms. A sizeable volume of research documented that EP habituation is not caused by the effector activity used in most studies to elicit the EP (Roemer et al., 1984). Therefore, scalp-recorded EPs should reflect intermediate processes such as sensory encoding and stimulus evaluation (Davis and Heninger, 1972). Probing P50 RS in a number of neuropsychiatric conditions has been shown to be a promising tool to help further our understanding of the neurobiological aberrations (Franks et al., 1983; Brockhaus-Dumke et al., 2008; Patterson et al., 2008) and genetic vulnerability (Adler et al., 1982; Siegel et al., 1984; Anokhin et al., 2007) associated with these conditions.

* Corresponding author. Address: Wayne State University, UPC-Jefferson, 2751 E. Jefferson, Suite 305, Detroit, MI 48207, USA. Tel.: +1 313 577 6687; fax: +1 313 577 5900.
E-mail address: nboutros@med.wayne.edu (N.N. Boutros).
[1] All data analyses.
[2] All data collection.

1388-2457/$36.00
http://dx.doi.org/10.1016/j.clinph.2012.10.007

Averaged EPs, recorded at the scalp following auditory stimulation, contain a temporal sequence of three major components subsequent to the brainstem auditory evoked responses: positive (P50), negative (N100), and positive (P200) deflections (Buchsbaum, 1977; Boutros and Belger, 1999). In RS experiments using the paired-stimulus paradigm (PSP), all three AERs are suppressed by stimulus repetition. The degrees to which the different AER amplitudes are suppressed with repetition are not correlated (Boutros et al., 2004a), and are therefore likely to be associated with distinct but possibly overlapping and interacting phases of RS. The study of RS in the human brain would benefit from the study of each component eventually leading to the elucidation of the entire system.

The PSP is widely used for examining RS (Smith et al., 1994; Rentzsch et al., 2008). When two identical stimuli (S1 and S2) are presented with a short interstimulus interval (ISI), the second P50 response is suppressed. This "P50 suppression" is thought to indicate habituation at a pre-attentive phase of information processing. Technically, suppression of the second stimulus is usually expressed as the S2/S1 ratio of the two P50 responses. As evidence of RS preceding the P50 stage of information processing is almost non-existent, it is likely that P50 RS represents the first or earliest stage of habituation of evoked responses in the CNS. Understanding this early phase of RS is essential for the eventual understanding of the entire process.

The most direct way to obtain a functional mapping of P50 RS would apply a combination of neuroimaging and intracranial P50 recording procedures directly from cortical regions in the same individuals as occurs in the presurgical evaluation of epilepsy (Spencer et al., 1997). The current study capitalized on the unique opportunity provided by treatment-resistant epileptic patients, who are being worked-up for therapeutic respective surgery, to map the amplitudes and RS of the P50 AER using data obtained from grid and strip electrodes placed on various areas of the cortex.

2. Materials and methods

Between 2001 and 2006, a total of 79 patients with drug-resistant focal epilepsies were implanted with cortical electrodes for invasive seizure recordings as part of their presurgical evaluation at the University of Bonn Epilepsy Surgery Center. Fifteen subjects were excluded due to extreme artifacts. Data presented here are from the remaining 64 subjects. There were 32 men, and ages ranged from 19 to 65 with a mean of 37 ± 12 years.

2.1. Patient characteristics and clinical methods

The standard diagnostic presurgical work-up included interictal and ictal video-electroencephalogram recordings with surface and subdural/depth electrodes to determine the exact location of seizure onset, and high-resolution MRI (Kral et al., 2002). Psychiatric status and history were assessed by an experienced psychiatrist (Boutros et al., 2006). It should be noted that psychiatric problems were minimal in this patient sample (Boutros et al., 2005). Of the 64 included subjects only 14 had any psychiatric history. None were diagnosed with either schizophrenia or bipolar disorders. The most frequent problems were history of depression or anxiety and none of the patients were on psychotropic medications at the time of recording. On the other hand, at the time of recording, all patients were on standard therapy with anticonvulsant drugs (AEDs). While in some patients AEDs were lowered to allow seizures to occur, none of the patients were completely off AEDs. Given that the number of electrodes exhibiting P50 responses at any one location varies between 4 and 18 and in view of the different AEDs used in different subjects, examination of the effects of individual AEDs on P50 and its gating was not attempted. Similarly, the possible effects of seizure variables (i.e., seizure frequency) were not attempted.

Of the 64 subjects, 30 had evidence of pathology on the right hemisphere, 25 on the left hemisphere and nine on both sides. Fourteen subjects had pathology localized to one of the medial temporal structures without evidence of neocortical lesions. RS experiments were performed after the individual invasive diagnostic program was finished, while patients were waiting for their therapeutic surgical procedure and/or electrode extraction. All patients signed an informed consent approved by both the University of Bonn and Wayne State University.

2.2. EP recording

All recordings were performed in a sound-shielded room which utilized a digital EPAS system (Schwarzer, Munich, Germany) and Harmonie EEG software (Stellate, Quebec, Canada). One hundred pairs of identical clicks were presented in a single session lasting about 14 min (S1 and S2; sinusoidal waves, frequency 1500 Hz, Gaussian envelope, duration 4 ms, onset and decay phase of 1.2 ms each) were presented binaurally via headphones with an interstimulus interval of 500 ms and an interpair interval of 8 s (Zouridakis and Boutros, 1992). No formal hearing examinations were performed. Patients reporting history of hearing difficulty were not included in the study. Prior to starting the recording procedure, hearing was tested clinically (equal hearing of a wrist watch and finger rubbing bilaterally). None of the subjects included had difficulties with these tests. Stimuli were presented binaurally via calibrated headphones with an intensity of 85 dB. This intensity has been found by this group to reliably generate P50 responses and not cause a startle reaction. Patients were asked to listen to the stimuli without additional tasks. Patients were asked to focus their gaze on a spot on the wall in front of them to minimize eye movements. They were encouraged to blink after they hear the second of the pair of stimuli (they had an interval of 8 s). An EEG technologist monitored the ongoing EEG to make sure subjects did not drift into drowsiness or sleep. Prior studies showed that only focused attention on the pairs of stimuli (e.g., counting odd pairs embedded among standard pairs) can influence the P50 response or its gating (Guterman et al., 1992; Jerger et al., 1992; Gjini et al., 2011). AERs were recorded from subdural strip and grid electrodes (sampling rate 1000 Hz per channel), with reference to both mastoids (the most common reference used for gating studies). Raw data were collected utilizing a band pass filter setting 0.03–85 Hz, 12 dB/octave. Prior to P50 analyses, data were further digitally filtered with a narrower bandpass filter of 1–45 Hz, with a notch filter for 50 Hz main line frequency noise (data collected in Germany). Data were segmented to epoch lengths of 500 ms, prestimulus baseline 100 ms. Details of electrode coverage were published in prior publications (Boutros et al., 2011). In brief, subdural electrodes consisted of strips or grids with stainless steel contacts with an interelectrode spacing of 1 cm (Behrens et al., 1994). An ECG electrode was glued to the patient shoulder for grounding purposes. In the extensive experience at the Bonn Epilepsy Center, this is the most convenient location and it had no effects on EEG recordings or source analysis. A figure showing all cortical regions where electrodes were placed has been previously published and is available online (Fig. S1 in the Supplementary Material of Boutros et al., 2011). Electrode placement was verified visually using post-implantation MRI with axial and coronal T2-weighted and FLAIR-sequences (slice thicknesses 2 and 3 mm, respectively) as well as sagittal T1-weighted sequences.

2.3. Signal processing

Due to the high signal to noise ratio attendant to direct cortical recordings and in view of the variability in the amplitudes of the recorded responses, no automatic artifact rejection parameters were employed. Post-hoc examination of the data showed that exclusion of epochs with the highest 10% amplitudes did not affect the averages. In fact it took deletion of 25% of the epochs before the averages began to change their morphologies. All contacts exhibiting P50 responses to S1 were identified by visual inspection of the resulting averaged waveform from a particular electrode. Occasional epileptic discharges were noted in the raw data. Overwhelmingly, those occurred in the 8 s interval between the pairs of stimuli. In the very rare occasion when an epileptic discharge occurred within the 600 ms interval including S1 and S2, this caused a significant change in the morphology of the resulting average which was then excluded due to the lack of the required morphology (an epileptic discharge being of negative potential and significantly larger than the relatively small positive potential P50 response). Given the rarity of this occurrence, no monitored brain region was excluded because of epileptic discharge occurrence. A two-step process was employed in order to increase the confidence that the identified components represent P50 responses to S1 stimuli. First we relied on the well-established scalp morphology of the Vertex Complex (i.e., P50/N100/P200) (Boutros et al., 2004b). The most prominent positive peak in the 35–80 ms time window following stimulus onset that clearly resembled the P50, as determined by two authors (KG and NNB) independently were subjected to the second analysis step. The segmented single-trial S1 responses (−100 to 400 ms) were baseline corrected by extracting the mean potential of the prestimulus interval (−100 to 0 ms). The averaged evoked responses were obtained and subsequently based on the average latency of the P50 peak and the previous trough, single trial peak-to-peak scores were extracted using these average latency values. Single trial peak-to-peak scores at baseline were also obtained by using the maximum positivity and negativity values in the −50 to 0 ms interval. Then t-statistics were obtained per each electrode by comparing peak-to-peak S1 evoked responses across trials by means of one-sample *t*-tests against zero. The same was done for the baseline peak-to-peak "noise" values. Finally, the *t*-value during the P50 peaking interval was compared with the *t*-value during the baseline period. The channel was marked as good when the *t*-value for P50 was numerically higher than the baseline respective value and as bad channel when vice versa. We didn't perform any correction for multiple comparisons here, because the intention was to apply some level of statistical thresholding in order to exclude only responses with low signal-to-noise ratio.

For the S2 response, a similar 2-step process was adopted but in a reverse order. Where an S1 response was selected (from the average), the segmented single-trial S2 responses (−100 to 400 ms) were baseline corrected as for the S1 responses. Then t-statistics were obtained per each electrode by comparing S2 evoked responses across trials by means of paired samples *t*-tests against zero. Finally, the *t*-value during the P50 peaking interval was compared with the *t*-value during the baseline period. For the S2, the channels were not labeled as good or bad like for the S1 but as response present or absent. For all channels with response present, P50 S2 components were visually identified. For channels with t-statistic indicating a non-significant difference from baseline, the averages were inspected visually by two investigators to determine if an S2 component could confidently be identified based on the morphology of the waveforms. If a P50 response to S2 could not be visually identified, the response was considered completely attenuated or suppressed and recorded as zero with an S2/S1 ratio of 0%. All visually identified P50 components were measured from peak to the preceding peak (Boutros et al., 2009). RS was quantified as the S2/S1 X 100 ratio with higher ratios indicating less effective RS. In patients exhibiting a P50 at several leads within an area (see below), the electrode with the largest P50 amplitude was chosen for the determination of the degree of RS in this region.

A table listing all the anatomical regions where electrodes were placed and the number of subjects with electrodes in this region was also previously published (Table S1 in the Supplementary Material of Boutros et al., 2011). The anatomical regions indicated were used as a guide to allow averaging of the data from closely related anatomical areas. Each designated area had a maximum of three electrodes. From each set of electrodes, the largest value was chosen to represent this area. A number of regions having more than three electrodes were arbitrarily divided into areas with only three electrodes. For example the ventral region of the Superior Frontal Gyrus (vSFG) was divided into two areas; v1SFG and v2SFG going from anterior to posterior.

2.4. Source localization

Only data from grids with a sufficient number of electrodes (minimum 64 electrodes) were used for source localization. As inter-electrode distance in intracranial electrode grids was 1 cm, the superficial cortical area covered by an 8-by-8 grid (i.e., 64 electrodes) was 64 cm^2. It is difficult to tell what would be considered a "sufficient number" of intracranial electrodes for source localization purposes; however three of the main factors that determined our selection were: (1) relatively large coverage of cortical areas; (2) regular inter-electrode spacing and coverage; and (3) increased probability for a presence of "sinks" and "sources" especially for coverages across major sulci. There were 20 subjects with this arrangement. Curry software (Compumedics Neuroscan Ltd.) was used for head modeling and source estimation. The sensor 3D positions were extracted from grids in post-implantation MRIs via identification of four corner electrodes and subsequent linear interpolation of electrode positions for the full array. To allow extended current patterns to be mapped, a weighted minimum-norm technique (LORETA: low resolution electromagnetic tomography (Pascual-Marqui et al., 1994) was used to estimate current density distributions from S1 signal P50 potentials and the difference waves (S1–S2). The difference wave is calculated by digitally subtracting the averaged S2 from the averaged S1 responses for each subject (Korzyukov et al., 2007; Arnfred, 2006). LORETA assumes that neighbor sources have similar strengths and allows reconstruction of smooth current distributions. LORETA applies the smoothness constraint based on the physiological assumption that neuronal activity in neighboring patches of cortex is correlated. Although the usefulness of implementation of this physiological constraint has been criticized based on the limited spatial resolution of EEG/MEG extracranial recordings, in our study we used intracranial data where sensors sit on top of major neuronal generators. As the distance between sensors and neuronal generators is drastically reduced, the effects of volume conduction are much less present in comparison with extracranially recorded EEG/MEG data. It might be also argued that closer distance between sensors and generators permits a finer resolution of distinct generators, in which case, volume conduction may be equally important for "far field" and "near field" recordings. While 1 cm electrode spacing is considered close for detecting far fields, it may not be so close when the underlying generators are near. Thus, the inverse problem is still potentially problematic for intracranial recordings. On the other hand, the volume conductor model (forward model) is simplified, and this is another advantage for intracranial versus extracranial recordings.

Individual BEM (boundary element model) head models were created from the subjects' MRI data and used to solve the forward problem. Segmentation of the MRI data was performed in order to

obtain the boundaries on the surface of the brain and inner skull that enclose tissue compartments which are assumed to be homogeneous and isotropic, with known conductivity values. A realistic head modeling routine in Curry software generated a high resolution discretisation of the surfaces with approximately 3500 nodes (about 2000 nodes representing the innermost brain compartment and about 1500 nodes for the CSF's BEM surface). As part of the distributed current density reconstructions with LORETA, the source locations were defined in the cortical surface (a source space which included thousands of locations and was defined by a sufficiently high sampling of the segmented cortical surface). A rotating source type was used instead of fixed source orientations (i.e. cortical surface normals) in order to allow estimation of omnidirectional currents and minimize the effects of nonoptimal surface segmentations. Noise level in the evoked responses was estimated from the pre-stimulus interval (−100 to 0 ms). The current density regularization parameter lambda (controlling the trade-off between data and the model) was optimized so that the residual deviation equaled 1/SNR (signal-to-noise ratio).

Optimal head modeling for intracranial data is still a matter of research (Acar and Makeig, 2010). The use of a single-compartment BEM model has been preferred (Fuchs et al., 2007) in conjunction with a spatially smoothed source space in order to avoid the issue whether grid cortical recordings allow reliable determination of source depth (Korzyukov et al., 2009). Here, we used a two-compartment BEM model (Cho et al., 2011) including the innermost brain and cerebrospinal fluid (CSF) compartments.

The sole purpose of source localization from grid electrodes was to show differences in terms of individual regions that are involved in both or predominantly in one of two studied processes, i.e., stimulus registration as reflected by the amplitudes of the responses to S1 and repetition suppression as reflected by the S1–S2 difference wave, during the P50 phase. This is important as one of the main working hypotheses is that the two functions are served by different neural circuitries.

2.5. Functional significance

Following identification of regions possibly contributing to P50 RS, the currently proposed functional significances of these regions were identified. For defining voxels of interest (VOIs), every grey matter voxel in the Montreal Neurological Institute (MNI) space (according to the tissue probability map templates) was assigned to the nearest electrode position. Hereby electrode location and hence the recorded effects could be related to standard stereotaxic space. For the functional characterization we proceeded as follows: using the BrainMap database (http://www.brainmap.org), all experiments that reported at least one focus of activation within each VOI volume were identified (Eickhoff et al., 2009, 2011). The functional characterization of each VOI was then based on the BrainMap metadata that describes the included specific mental process isolated by the statistical contrast of each included experiment. Behavioral domains (BD) include the main categories of cognition, action, perception, emotion, interoception, as well as their related subcategories. The respective paradigm classes (PC) classify the specific task employed (a complete list of BDs and PCs can be found at http://www.brainmap.org/scribe/). We analyzed the behavioral domain and paradigm class metadata associated with each identified VOI to determine the frequency of domain "hits" relative to its likelihood across the entire database (Eickhoff et al., 2010). In particular, functional roles of the derived clusters were identified by significant over-representation of BDs and PCs in the experiments activating the respective cluster relative to the BrainMap database using a binomial test ($p < 0.05$), corrected for multiple comparisons using Bonferroni's method (Laird et al., 2009a,b).

3. Results

Means and standard deviations of P50 amplitudes in the 10 brain regions exhibiting the largest P50 amplitudes and where at least three subjects had electrodes are presented in Table 1. The requirement that at least three subjects be represented allowed the calculations of a standard deviation for each location. Where the standard deviation was equal to or larger than the mean (indicating a significant degree of variability), the data were not included. The recorded P50 components are unlikely to reflect passive volume conduction as contiguous regions showed highly different amplitudes as seen in Fig. 1.

Of the 127 cortical regions sampled, 56 regions exhibited significant activity in the P50 latency range as compared to the pre-stimulus baseline. The largest amplitudes were noted on the dorsal most part as well as the middle regions of the right Superior Temporal Gyrus (r-STG) followed by two parietal regions; the inferior-dorsal part of the right Inferior Parietal Gyrus (r-IPG) and the interior-dorsal part of the left Inferior parietal Gyrus (l-IPG). The next six highest amplitude regions included the dorsal regions of the left Middle Temporal Gyrus (l-MTG) and the left Superior Temporal Gyrus (l-STG), two adjacent regions (posterior and middle ventral) of the left cingulate gyrus and the middle-dorsal area of the right cingulate gyrus, and the dorsal region of the right Middle Parietal Gyrus (r-MPG) (Fig. 1). Thus four of the ten highest amplitude P50 regions were in the temporal cortex, mainly the STG. Three parietal (mostly IPG), and three cingulate area regions (mostly middle regions) also exhibited high amplitude P50 responses. Fig. 1 shows the grand averages of the evoked responses obtained from the ten regions with the most prominent P50 responses.

Paired-samples *t*-tests were utilized to assess the number of sampled brain regions with significant P50 responses to S1 and exhibiting significant RS of those P50 responses at a significance level of $p < 0.05$. All 56 regions exhibiting significant P50 activity also showed RS of the S2 responses. In none of the 56 regions were S2s equal to or larger than S1 amplitudes (i.e., no RS). The degree of RS nonetheless varied widely among the 56 regions. Of these 56 regions, 23 exhibited a significant decrease in the amplitude of the responses to S2 stimuli. The ten lowest P50 RS ratios (strongest P50 RS) derived from the different brain regions are given in Table 2. This table also lists the ten regions with least RS of the P50 (highest ratios). It should be noted that the RS ratios did not significantly differ among the listed high RS or among the listed low RS regions. The table thus represents a listing of the regions exhibiting most and least RS. The strongest P50 RS was recorded from electrodes overlying the middle-dorsal area of the right cingulate gyrus and the ven-

Table 1
Ten cortical regions with largest amplitudes P50 in μV.

Region (number of subjects)	Min Amp	Max Amp	Mean and SD
RtdSTG (9)	3.9	78.3	37.9 ± 20
Rt-mdSTG (8)	7.8	60	24.7 ± 20
Rt-idlPG (4)	11	43	24.7 ± 13.5
Lt-idlPG (5)	5.7	55	24.4 ± 18
Lt-dMTG (18)	6.9	60	23.5 ± 14.7
Lt-pCing (3)	15.4	29.6	22.1 ± 7.1
Lt-vmdCing (5)	9.1	36.8	21.9 ± 9.9
Lt-dSTG (13)	6.9	37.7	19.1 ± 9.6
Rt-dmdCing (5)	4.6	29.4	19.2 ± 10.5
Rt-dMPG (3)	8.1	37.5	19.1 ± 16

Lt, left; Rt, right; Rt-dSTG, dorsal superior temporal gyrus; Rt-mdSTG, mid-dorsal superior temporal gyrus; Rt-idlPG, inferior dorsal inferior parietal gyrus; Lt-idlPG, inferior dorsal inferior parietal gyrus; Lt-dMTG, dorsal middle temporal gurus; Lt-pCing, posterior cingulate gyrus; Lt-vmdCing, ventral middle cingulate gyrus; Lt-dSTG, dorsal superior temporal gyrus; Rt-dmdCing, dorsal middle cingulate gyrus; Rt-dMPA, dorsal middle parietal area.

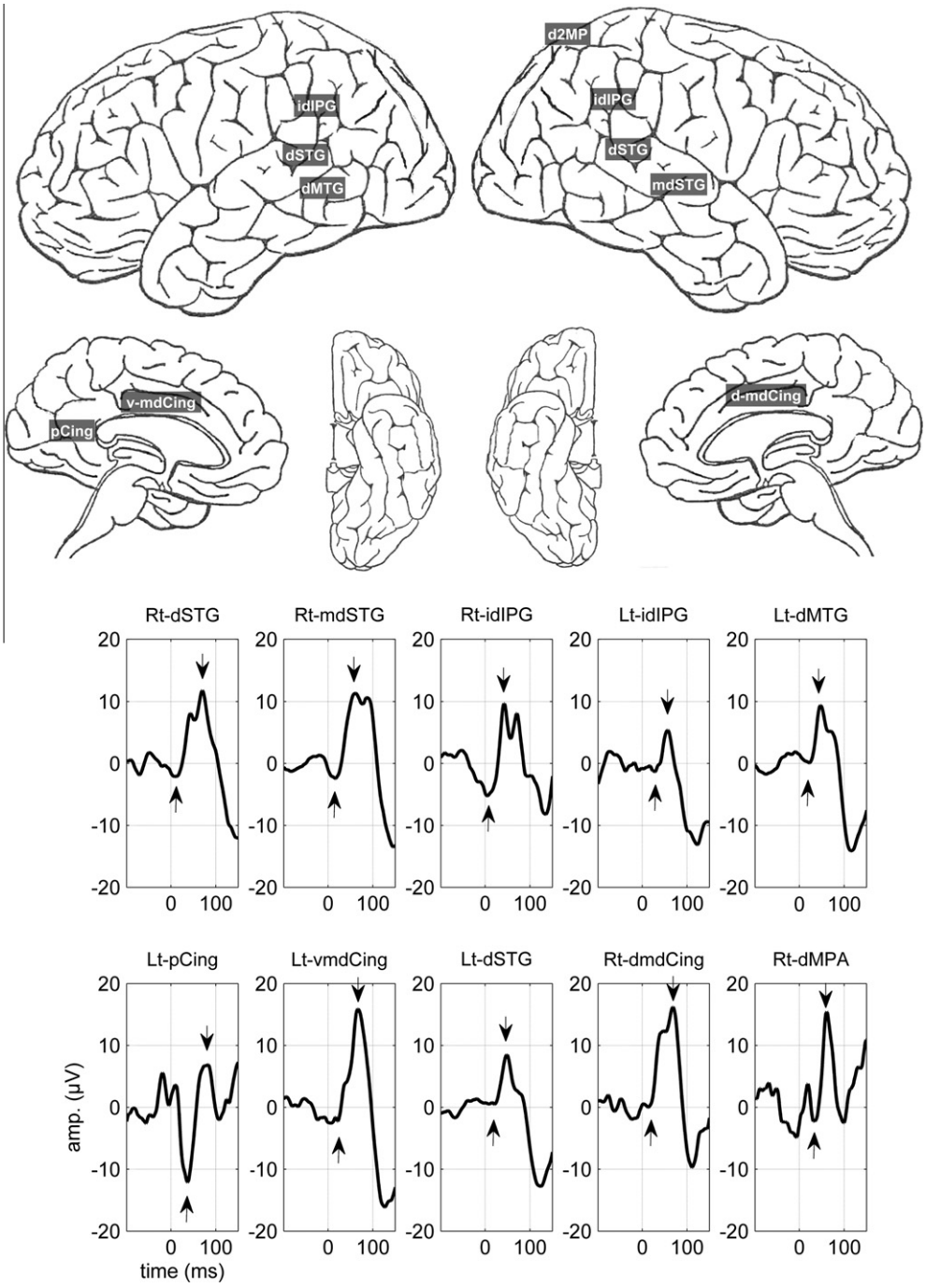

Fig. 1. Cortical regions exhibiting the largest amplitude P50s and the grand averages of each region. For abbreviations please refer to Table 1 legend.

tral area of the right MTG. Strong P50 RS was also noted from the dorsal right Superior Frontal Gyrus (r-SFG), superior-ventral region of left occipital lobe, inferior/ventral area of the right Inferior frontal Gyrus (r-IFG), the middle region of the right IPG, and the dorsal region of the right STG. Also among the ten regions exhibiting strongest P50 RS were the dorsal area of the right Middle Frontal Gyrus (r-MFG), the inferior-middle area of the right Inferior Frontal Gyrus (r-IFG), and the dorsal area of the left middle Frontal Gyrus (l-MFG). So while four of the highest P50 amplitude regions were temporal, only two temporal regions exhibited strong RS, of which only one region (r-STG) exhibited both high amplitude P50s and strong RS. On the other hand, while no frontal lobe regions were represented among the high amplitude P50 response area, five frontal lobe regions exhibited strong P50 RS. One cingulate region also exhibited both high amplitude P50 responses and strong RS (right middle-dorsal).

Regions with the least RS (Table 2 and Fig. 2) included the ventral area of the right MFG, inferior-ventral area of the left IPG, superior-ventral area of the right occipital lobe, and the dorsal area of the left Inferior Temporal Gyrus (l-ITG). Also among cortical regions exhibiting minimal P50 RS were ventral area of the left MFG, the middle areas of the right and left ventral medial temporal lobe, dorsal area of right ITG, middle area of the left STG, and the left posterior cingulate region. Only one region exhibited both high amplitude P50 responses and weak RS, namely the left posterior cingulate region. It should be noted that five of the least P50 RS

Table 2
Ten regions with strongest (smaller ratios) and ten with weakest (larger ratios) gating of the P50 (S2/S1 X 100).

Strong RS regions	Mean and SD	Functional significance
Rt-dmdCing (5)	11 ± 30	Action: imagination, execution; tasks: anti-saccades, finger tapping, flexion/extension, imagined movement, saccades
Rt-vMTG (3)	18 ± 15	Emotion: happiness, disgust
Rt-dSFG (4)	21 ± 16	Action: imagination, motor learning; visual perception: motion; tasks: action observation, anti-saccades, drawing, finger tapping, flexion/extension, imagined movement, mental rotation, saccades, sequence recall/learning, visual distractor/visual attention
Lt-svOL (4)	24 ± 40	Cognition: language, memory, music, reasoning; tasks: counting/calculation, Sternberg task
Lt-ivIFG (4)	27 ± 28	Emotion: disgust; cognition; tasks: delayed match to sample, eating/drinking, reward task
Rt-imdIPG (4)	28 ± 13	Action; perception; task: visual distractor/visual attention
Rt-dSTG (9)	29 ± 20	Perception; tasks: action observation, face monitor/discrimination, film viewing, music comprehension/production, oddball discrimination, passive listening, pitch monitor/discrimination, reading (overt), tone monitor/discrimination.
Rt-dMFG (4)	29 ± 7	Action: execution, imagination; perception; tasks: finger tapping, flexion/extension, imagined movement, saccades, tactile monitor/discrimination
Rt-imdIFG (6)	30 ± 29	Action: imagination, inhibition; interoception: air-hunger, sleep, thirst; emotion; tasks: flexion/extension, non-painful electrical stimulation, oddball discrimination, pain monitor/discrimination, tactile monitor/discrimination, tone monitor/discrimination
Lt-dMFG (6)	39 ± 32	Action execution: other than speech; perception: somesthesis (other than pain); tasks: finger tapping, go/no-go, grasping, imagined movement, non-painful electrical stimulation, sequence recall/learning, tactile monitor/discrimination, vibrotactile monitor/discrimination, visual distractor/attention
Weak RS regions		
Rt-vMFG (3)	89 ± 67	Cognition: attention, memory, reasoning; tasks: counting/calculation; delayed match to sample, Sternberg task, task switching, visual distractor/visual attention
Lt-ivIPG (5)	86 ± 39	Action: execution; perception: audition, somesthesis (pain); tasks: finger tapping, non-painful electrical stimulation, oddball discrimination, pain monitor/discrimination, passive listening, tactile monitor/disrimination, tone monitor/discrimination, chewing/swallowing
Rt-svOL (4)	85 ± 78	Cognition; perception; tasks: action observation, film viewing, saccades, visual distractor/visual attention, visual pursuit/tracking
Lt-dITG (5)	80 ± 76	Cognition: language (orthography, semantics); tasks: face monitor/discrimination, reading (covert, overt), semantic monitor/discrimination
Lt-vFMG (4)	77 ± 16	Cognition: attention, memory, reasoning; tasks: delayed match to sample, semantic monitor/discrimination, Sternberg task, task switching, word generation (overt, covert), n-back
Rt-mdmT (8)	76 ± 35	Emotion: anger, fear; interoception: air-hunger, bladder, sexuality; tasks: face monitor/discrimination; olfactory monitor/discrimination, passive viewing, reward task
Rt-dITG (7)	67 ± 35	Emotion; cognition; face monitor/discrimination
Lt-mdmT (7)	64 ± 40	Emotion: fear, anxiety, disgust; interoception: air-hunger, sexuality, sleep, thermoregulation; tasks: cued explicit recognition, face monitor/discrimination, naming (overt), passive viewing
Lf-mdSTG (11)	60 ± 48	Action; cognition; emotion; tasks: drawing, oddball discrimination, passive listening, phonological discrimination, pitch monitor/discrimination, reading (overt), recitation/repetition (overt), syntactic discrimination, tone monitor/discrimination, chewing/swallowing
Lt-pCing (3)	55 ± 32	Cognition: attention, memory, reasoning; tasks: flashing checkerboard, visual pursuit/tracking

dmdCing, dorsal middle cingulate gyrus; vMTG, ventral middle temporal gyrus; dSFG, dorsal superior frontal gyrus; svOL, superior ventral occipital lobe; ivIFG, inferior ventral inferior frontal gyrus; imdlPG, inferior middle inferior parietal gyrus; dSTG, dorsal superior temporal gyrus; dMFG, dorsal middle frontal gyrus; imdlFG, inferior middle inferior frontal gyrus; dMFG, dorsal middle frontal gyrus; vMFG, ventral middle frontal gyrus; ivIPG, inferior ventral inferior parietal gyrus; svOL, superior ventral occipital lobe; dITG, dorsal inferior temporal gyrus; vMFG, ventral middle frontal gyrus; mdmT, middle medial temporal area; dITG, dorsal inferior temporal gyrus; mdSTG, middle superior temporal gyrus; pCing, posterior cingulate gyrus.

regions were temporal. Table 2 lists the currently proposed functional significances of both strong and weak RS regions. Fig. 2 shows the ten cortical regions exhibiting maximal gating of the P50 and the ten regions exhibiting the least gating and the evoked responses (S1 and S2 averages) from each region. It should be noted that the averaged EPs do not exactly match the means of the individual evoked responses. This discrepancy is secondary to the effects of latency variability which is not taken into account when calculating the mathematical means. A wider discrepancy would thus reflect more variable latencies of the components recorded from this site. The discrepancy is most prominent in relation to S2 averages due to larger tendency towards latency variability. As can be seen from Fig. 2, the graphs for the grand averages obtained from the right-superior-ventral occipital and the left posterior cingulated regions indicate strong attenuation of S2 when in fact the mathematical means indicate very weak RS.

Source reconstruction from grid data over the lateral surface of the left hemisphere localized P50 generators for the S1 signal in the STG areas (in four of six grid placements encompassing the left lateral sulcus), in the posterior part of SFG (two of five cases with coverage for that area), left inferior parietal cortex (four of six cases) and left ventral prefrontal cortex (two of six cases). RS generators from the difference wave (S1–S2) P50 potentials localized to the posterior part of SFG (four of five cases), the left ventral prefrontal cortex (three of six cases with that area coverage), left inferior parietal cortex (four of six cases), and the posterior part of STG (in three of six grid placements encompassing the left lateral sulcus) (Fig. 3: Subjects 15 and 19, and Supplementary Fig. S1).

For subjects with grids placed over the lateral surface of the right hemisphere, P50 generators for the S1 signal were localized in STG areas (in five of seven grid placements encompassing the right lateral sulcus), in the SPG area (in two of six grid placements covering that area), inferior parietal (in five of seven cases), and the posterior part of SFG (two of three cases) cortices. RS generators for P50 S1–S2 difference wave potentials were localized in STG areas (in six of seven cases with respective grid coverage), the SPG area (three of six cases), inferior parietal cortex (in five of seven grid placements), the posterior part of SFG (two of three cases), and the right ventral frontal area (one case) (Fig. 3: Subject 1, and Supplementary Fig. S1).

4. Discussion

This study represents a survey of brain regions, monitored for the purpose of localization of epileptic lesions, for their initial response to auditory stimuli and the degree to which they exhibit RS and can be considered likely contributing to sensory gating function in the preattentive phase of information processing. As expected the temporal cortices exhibited robust P50 components (Liégeois-Chauvel et al., 1994; Grunwald et al., 2003; Korzyukov et al., 2007). From the 10 regions exhibiting the largest P50 ampli-

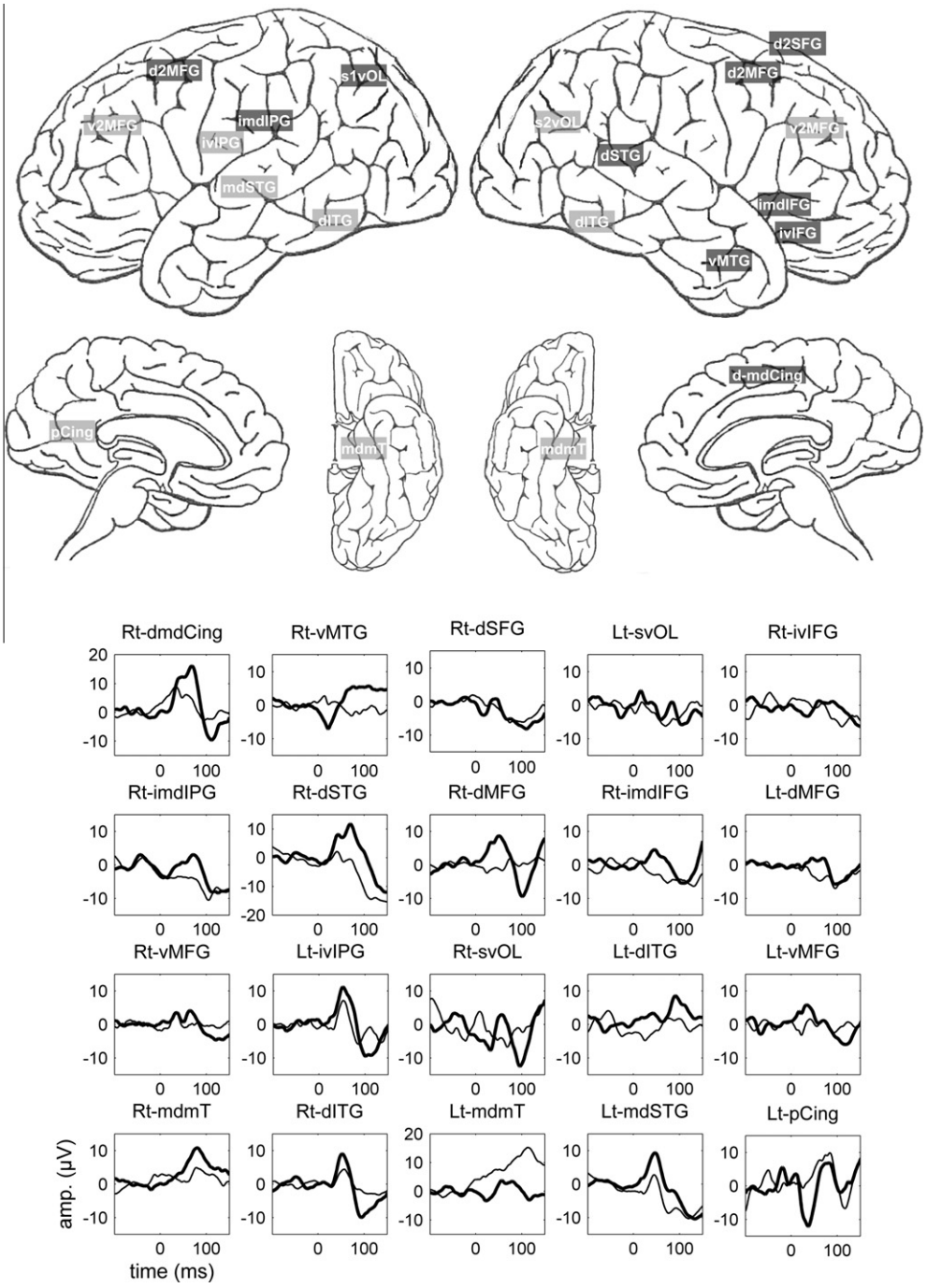

Fig. 2. The ten cortical regions exhibiting maximal gating of the P50 (dark shaded regions) and the ten regions exhibiting the least gating (light shaded areas) and the evoked responses (S1-thick line and S2-thin line) from each region. For abbreviations please see Table 2 legend.

tudes, four were temporal, three parietal, and three cingulate while five of the ten regions exhibiting strong P50 RS were prefrontal regions. Among the prefrontal regions involved were: the dorsal region of the right SFG, the middle and ventral areas of the right IFG, and the dorsal areas of the left and right MFGs. This is an important observation as no frontal regions were among the 10 areas exhibiting largest amplitude P50s. The data thus support a significant role of the frontal lobes in mediating P50 RS (Weisser et al., 2001; Korzyukov et al., 2007; Weiland et al., 2008; Garcia-Rill et al., 2008). The data also suggest that the parietal and cingulate regions are involved in both stimulus registration (S1) and P50 RS. A number of parietal and cingulate regions exhibited large P50s and strong RS. To our knowledge, this is the first report suggesting the involvement of both regions either in the generation of the P50 response or its RS.

The data strongly suggest that S1 amplitude and RS reflect two distinct functions that are served by different neural circuitries. This assertion is born out from the difference of the topography of the S1 and the S1–S2 difference wave seen in Fig. 3 and Supplementary Fig. S1. It should be underlined that data derived from grid electrodes are limited to the locations of the electrodes and do not fully reflect activity from other brain regions. Based on our recent work (Fuerst et al., 2007; Chang et al., 2011), and others (Shan et al., 2010) we believe that the ratio measure (which could not be used for source reconstruction) is more closely linked to S2 while the difference measure is more closely related to S1 ampli-

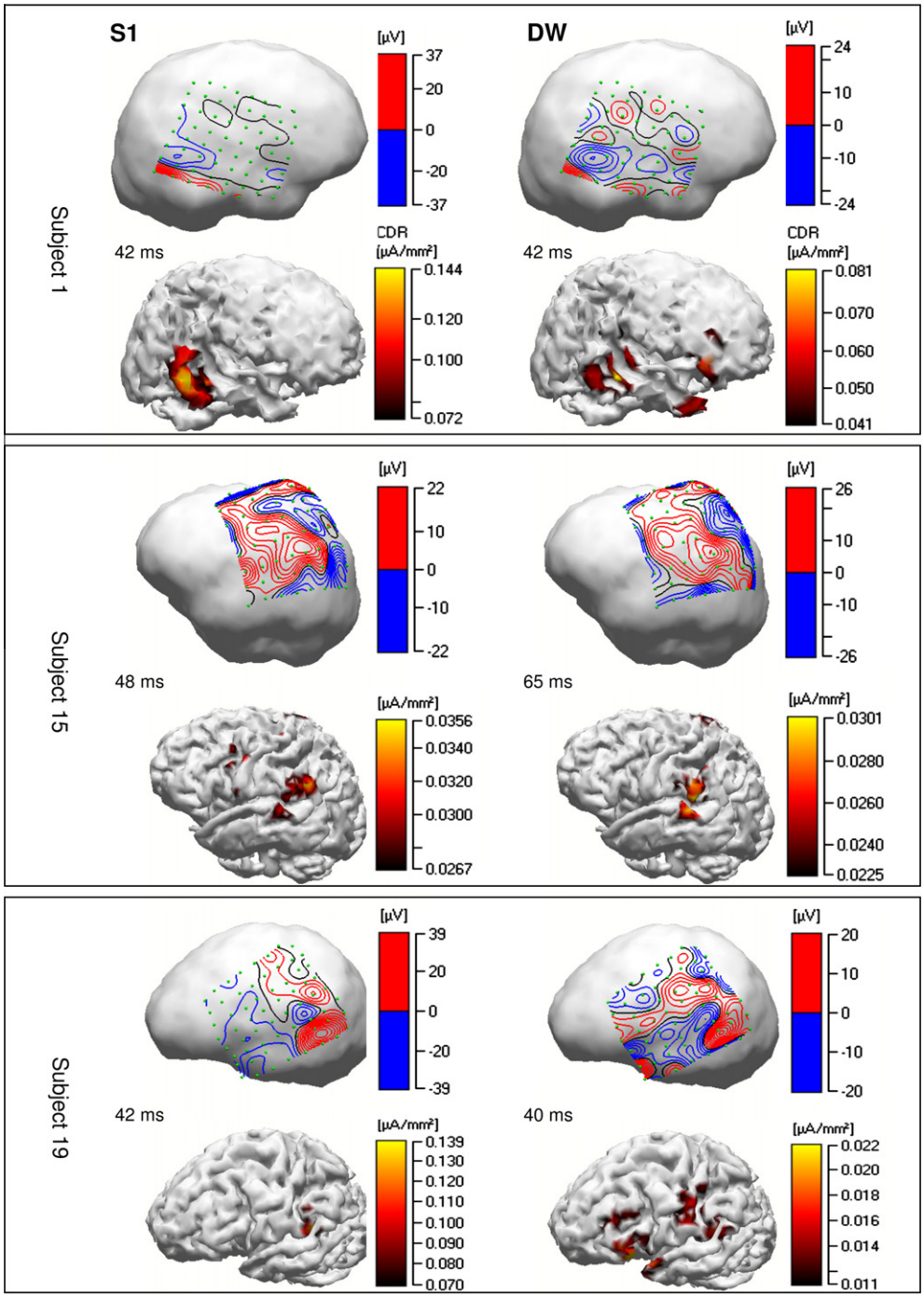

Fig. 3. Topographies of the cortical potentials and estimated current densities for three selected subjects (out of 20) showing differences in cortical potential distributions and generators of S1 signal P50 potential (stimulus registration) and S1–S2 difference waves (sensory gating). Differences are mostly shown in terms of individual regions that are involved in both (subject 15) or predominantly in one of two studied processes such as stimulus registration and repetition suppression (subjects 1 and 19). Data from 20 subjects are shown in the Supplementary Materials section. DW, difference wave; CDR, current density reconstruction.

tudes. Hence, we believe that the ratio measure more closely reflects the phenomenon under investigation (i.e., RS). The main purpose of providing the source localization data was to underscore the fact that the two phenomena (i.e., amplitude of the P50 response to S1 stimuli and the degree of attenuation of the P50 response to S2 stimuli) are indeed different functions and possibly mediated by different circuitries. By employing the S1–S2 difference, which (as noted) is more closely linked to S1 (Atchley et al., 1976), we may have underestimated the degree of difference between the two functions. Given that the two topographies did not completely overlap in our sample, we felt that the data supported our hypothesis.

While the data suggest that both parallel and serial processing are involved in mediating RS, methodology like dynamic causal modeling may be necessary to directly examine the nature of the interaction between the different regions identified as potentially involved in RS (Grau et al., 2007).

In a prior report examining N100 RS (Boutros et al., 2011), we advanced the possibility that areas with the least RS may be important for RS as some regions must remain responsive in order for the

brain to be able to evaluate all incoming stimuli. Among the 10 least P50 RS regions five were temporal. Two frontal regions exhibited low P50 RS: the ventral areas of the right and left Middle Frontal Gyri. Moreover, regions with the strongest observed P50 RS were mainly on the right side (eight of ten regions) while large amplitude P50 and weak P50 RS regions were more equally distributed between the two hemispheres. These observations suggest that while the temporal lobe is paramount for the initial registration of the sensory input, it is the frontal lobe (and perhaps the right frontal cortex) that determines the responses were the stimulus to be repeated.

Similar to the N100 response, the temporal lobes (particularly the STG) contributed heavily to the generation of the initial response (i.e., response to S1) and also similar to the N100 response with significant contributions from the parietal and cingulate regions. The exact significance of the extra-temporal contributions is currently unknown. Again, similar to the N100, a significant number of prefrontal lobe regions (with fewer regions from cingulate and parietal areas), exhibited strong P50 RS and are likely to be playing significant roles in the RS of the pre-attentive P50 response.

Two significant differences emerge between RS of the P50 and N100 responses. First, whereas three frontal pole areas exhibited no RS of the N100 response (and thus are subject to further investigation of their possible role in RS of the N100), no frontal pole regions were among the least P50 RS regions. Secondly, whereas no hemispheric predominance was observed in any N100 related variables, seven of the ten strongest P50 RS regions were from the right hemisphere. These observations overall suggest that the P50 and N100 responses are different aspects of one RS system with different but likely overlapping functions. The elucidation of the exact function or aspect of the overall brain's RS capability each component reflects requires further and more targeted investigations.

Sable et al. (2004) provided evidence that RS is not a simple matter of refractoriness but more likely reflects an active inhibitory process. This view was earlier challenged (Budd et al., 1998) relating the degree of attenuation to the degree of refractoriness based on the closeness of stimulus repetition. Jääskeläinen et al. (2004) provided strong evidence from combined EEG/MEG recordings from healthy individuals of a specific role for the posterior auditory cortex in RS of repeating sounds due to transient adaptation of feature-specific neurons within this region. It is important to highlight the fact that while the strongest RS areas were outside the STG, the STG exhibited significant P50 RS from 35% to 60% which is similar to what is reported in the literature (Hanlon et al., 2005). Published MEG studies to date have not attempted to compare as many different cortical regions similar to what is provided here from direct cortical recordings.

Based on the functional significances derived from correlations between functional studies and the MNI idealized MRI, different patterns of proposed functional significance emerge for the strong vs. weak P50 RS regions (Table 2). Five of the ten strongest P50 RS areas are concerned with action and execution of different tasks while six of the ten weakest P50 RS areas are concerned with different aspects of cognition. This observation further suggests that these brain areas (strong RS vs. weak RS) may be playing complementary roles in the overall RS process. Furthermore, the subtle differences between the functionalities of the P50 and N100 strong RS regions could also prove significant. Similar to the P50, six of the strongest N100 RS regions were concerned with action and execution of different tasks. The difference appears in the other strong RS areas: whereas for the P50, the other strong RS regions are concerned with emotions and perception, for the N100 they were mainly concerned with cognition. This observation may underscore the hypothesis that the RS P50 functions are bottom-up preattentive in nature while the N100 RS functions are more top-down early attentive processes.

The currently proposed model for P50 RS is centered on the CA3 region of the hippocampus and suggests that the first stimulus (S1) activates both the pyramidal cells and the inhibitory interneurons. Upon arrival of the second stimulus (S2) the inhibitory interneuron being still active, prevents or attenuates the response from the pyramidal cells (Freedman et al., 1996; Moxon et al., 2003). The model is too simple as RS has been shown to be multistage (Boutros and Belger, 1999; Gjini et al., 2010). A number of regions have been identified to be involved in RS in general. Central among these are the temporal neocortex and hippocampus. The exact role of the hippocampus in mediating RS of the P50 response is not clear. Our prior data from direct recording from the hippocampal and rhinal regions of epilepsy patients did not reveal clear hippocampal activation during the P50 time frame (Grunwald et al., 2003; Boutros et al., 2005) Subsequent further analysis of the hippocampal/rhinal data showed some activity limited to the posterior hippocampal region during the P50 time frame thus keeping the possibility of a role for the hippocampus in RS of the P50 response possible (Boutros et al., 2008).

Accumulating evidence strongly points to the prefrontal cortex as crucial to this function. It is thus possible to consider these three regions (temporal neo-cortex, pre-frontal cortex and hippocampus) as the nuclear auditory RS apparatus. Most prominent among other brain regions that have been implicated in RS, is the thalamus, particularly the reticular nucleus (nRT) (Krause et al., 2003). The involvement of the thalamus was also supported by observation of worsening of somatosensory RS in patients with thalamic strokes with recovery of the function over time (Stains et al., 2002). Other regions implicated include the amygdala (Cromwell et al., 2005; Cromwell and Woodward, 2007), which was proposed to be important in mediating rapid auditory sensory processing involved in emotional conditioning. The current study further identifies parietal and cingulate regions as likely contributors perhaps modulating the nuclear three-site circuit. It is currently not known if activity in one stream (auditory, visual or somatosensory) influences RS in other systems. However, it is likely that activity in one system is not completely independent from activity in other systems and perhaps explaining the significant involvement of the parietal and occipital cortices with auditory RS experiment. Our prior work points to a supramodal role for the prefrontal cortex in mediating RS (Bowyer et al., 2007). The above data also implicated the cingulate region. We now postulate that the cingulate and parietal regions are engaged in the RS of the P50 response at a preattentive phase of information processing. As there is some evidence of frontal activation around the P50 time frame, we can postulate that it is involved in the pre-attentive phase. It is possible to hypothesize a role for the thalamus at the junction between the preattentive (bottom up) RS process and the early attentive stages (or beginning of a top-down phase) of sensory RS. This role is crucial as the progress between these two phases is likely to depend on the proper recruitment of the other structures that has been implicated in RS like the hippocampus, cingulate, and the amygdala.

It should be acknowledged that simulation studies are required in order to critically evaluate the influence of several factors such as intracranial electrode distance, area coverage, inclusion or not of other "spatially limited" sensor information from electrode strips along with data from large grids comprised of equidistant electrodes, and for selection of the best source localization algorithm (i.e. LORETA versus dipole fitting, beamformer imaging etc.). As mentioned in the methodology section, the source space was defined by a sufficiently high sampling of the segmented cortical surface and a rotating source type was chosen in order to allow estimation of omnidirectional currents and minimize the effects of nonoptimal surface segmentations. Especially in situations where more than one generator of the studied response is present, the selection of a distributed source localization method

such as LORETA is advantageous versus single/multiple dipole fitting and beamformer algorithms, as well as un-weighted minimum norm solutions (bias towards superficial sources).

Along with well-known sources located in bilateral temporal and lateral frontal regions from traditional EEG/MEG source localization methodologies, evidence for additional sources contributing to P50 generation is provided by evoked potentials obtained from electrode strips over medial parts of both hemispheres (such as cingulate gyri), where we noticed the presence of large responses with high SNR. Following a traditional source localization methodology from EEG/MEG extracranial data, these highly active generators could be unnoticed or considered as ghost sources in the presence of bilateral temporal and other lateral sources. In addition, the issue of "volume conduction" regarding the presence or absence of parietal generators was better addressed using LORETA methodology on large grids with coverage of lateral parietal and superior temporal areas.

It should also be acknowledged that utilizing data from individuals with significant brain pathology (like in subjects with intractable seizures) places serious limitations on the overall interpretation of the results. While we elected to merge all participants as one group, it is likely that some of the data were influenced by the laterality of the pathology. However, our prior investigation of this possibility did not yield any major findings (Rosburg et al., 2008). Also, psychopathology was minimally represented in this group (Boutros et al., 2006). On the other hand, this patient sample provides the only possibility of directly examining RS from data recorded directly from many cortical regions. As the intent of the work was to define the network sub-serving normal RS, one cannot be completely assured of how close the data comes to reflecting what is being sought. Once technology advances to allow closer examination of cortical activity, it would be of significant interest to see if the data remains compatible with data provided here. If in fact, the data significantly differs, this could possibly be interpreted to reflect effects of epilepsy on the process of RS which would also be of interest to this field of research. Another limitation of the employed methodology is that the sampling of brain areas is not based on hypotheses by dictated by the clinical situation of the individual subjects. As much as this can be mitigated by the large sample size, there are salient regions that are never sampled using this patient sample, most prominently the thalamus. Finally, given the large number of brain regions sampled, the possibility of a type-I error (false positive) exists. As the main purpose of this work (given all the above limitations) was to help guide future imaging or dense electrode scalp data studies by providing candidate regions of interests (ROIs), our *t*-tests were not corrected for multiple comparisons. We felt that Bonferroni correction, in particular, would be too strict for this purpose.

While the work described in this report was largely motivated by the desire to more fully describe the neural circuitry underlying RS of the P50 (i.e. the preattentive phase of RS), in order to further our understanding of the RS problem in schizophrenia, the work may also have implications for epilepsy. As for psychiatric populations, thorough knowledge of this system could guide the development of more targeted pharmacotherapy as well as guide focal therapeutic procedures like transcranial magnetic stimulation (TMS) or deep brain stimulation (DBS). As for epilepsy, if future work proves that data provided here were strongly influenced by the epileptic process, this information would shed much needed light on the interrelationship between epilepsy and co-morbid psychopathology.

Financial disclosure

The authors reported no biomedical financial interests or potential conflicts of interest.

Acknowledgements

This work was supported by the National Institutes of Health (RO1 MH063476) and the Joe Young funds from the Department of Psychiatry and Behavioral Neurosciences, Wayne State University.

Appendix A. Supplementary data

Supplementary data associated with this article can be found, in the online version, at http://dx.doi.org/10.1016/j.clinph.2012.10.007.

References

Acar ZA, Makeig S. Neuroelectromagnetic forward head modeling toolbox. J Neurosci Methods 2010;190:258–70.
Adler LE, Pachtman E, Franks RD, Pecevich M, Waldo MC, Freedman R. Neurophysiological evidence for a defect in neuronal mechanisms involved in sensory gating in schizophrenia. Biol Psychiatry 1982;17:639–54.
Anokhin AP, Vedeniapin AB, Heath AC, Korzyukov O, Boutros NN. Genetic and environmental influences on sensory gating of mid-latency auditory evoked responses: a twin study. Schizophr Res 2007;89:312–9.
Arnfred SM. Exploration of auditory P50 gating in schizophrenia by way of difference waves. Behav Brain Funct 2006;28:2–6.
Atchley WR, Gaskins CT, Anderson's D. Statistical properties of ratios. I. Empirical results. Syst Zool 1976;25:127–48.
Behrens E, Zentner J, van Roost D, Hufnagel A, Elger CE, Schramm J. Subdural and depth electrodes in the presurgical evaluation of epilepsy. Acta Neurochir (Wien) 1994;128:84–7.
Boutros NN, Belger A. Midlatency evoked potentials: attenuation and augmentation reflect different aspects of sensory gating. Biol Psychiatry 1999;45:917–22.
Boutros NN, Korzyukov O, Jansen B, Feingold A, Bell M. Sensory-gating deficits during the mid-latency phase of information processing in medicated schizophrenia patients. Psychiatry Res 2004a;126:203–15.
Boutros NN, Korzyukov O, Oliwa G, Feingold A, Campbell D, McClain-Furmanski D, et al. Morphological and latency abnormalities of the mid-latency auditory evoked responses in schizophrenia: a preliminary report. Schizophr Res 2004b;70:303–13.
Boutros NN, Trautner P, Rosburg T, Korzyukov O, Grunwald T, Schaller C, et al. Sensory gating in the human hippocampal and rhinal regions. Clin Neurophysiol 2005;116:1967–74.
Boutros NN, Trautner P, Rosburg T, Korzyukov O, Grunwald T, Schaller C, et al. Mid-latency auditory evoked responses and sensory gating in focal epilepsy. J Neuropsychiatry Clin Neurosci 2006;18:409–16.
Boutros NN, Mears R, Pflieger PE, Moxon KA, Ludowig E, Rosburg T. Sensory gating in the human hippocampal and rhinal regions: regional differences. Hippocampus 2008;18:310–6.
Boutros NN, Brockhaus-Dumke A, Gjini K, Vedeniapin A, Elfakhani M, Burroughs S, et al. Sensory-gating deficit of the N100 mid-latency auditory evoked potential in medicated schizophrenia patients. Schizophr Res 2009;113:339–46.
Boutros NN, Gjini K, Urbach H, Pflieger ME. Mapping repetition suppression of the N100 evoked response to the human cerebral cortex. Biol Psychiatry 2011;69:883–9.
Bowyer SM, Boutros N, Korzyukov O, Tepley N. Supra-modal role for frontal cortex in sensory gating. Int Congr Ser 2007;1600:367–70.
Brockhaus-Dumke A, Schultze-Lutter F, Mueller R, Tendolkar I, Bechdolf A, Pukrop R. Sensory-gating in schizophrenia: P50 and N100 gating in antipsychotic-free subjects at risk, first-episode and chronic patients. Biol Psychiatry 2008;64:376–84.
Buchsbaum MS. The middle evoked response components and schizophrenia. Schizophr Bull 1977;3:93–104.
Budd TW, Barry RJ, Gordon E, Rennie C, Michie PT. Decrement of the N1 auditory event-related potential with stimulus repetition: habituation vs. refractoriness. Int J Psychophysiol 1998;31:51–68.
Chang WP, Arfken C, Boutros NN. Probing the relative contribution of the first and second responses to sensory gating indices: a meta-analysis". Psychophysiology 2011;48:180–92.
Cho JH, Hong SB, Jung YJ, Kang HC, Kim HD, Suh M, et al. Evaluation of algorithms for intracranial EEG (iEEG) source imaging of extended sources: feasibility of using iEEG source imaging for localizing epileptogenic zones in secondary generalized epilepsy. Brain Topogr 2011;24:91–104.
Cromwell HC, Anstrom K, Azarov A, Woodward DJ. Auditory inhibitory gating in the amygdala: single-unit analysis in the behaving rat. Brain Res 2005;1043:12–23.
Cromwell HC, Woodward DJ. Inhibitory gating of single unit activity in the amygdala: effects of ketamine, haloperidol, or nicotine. Biol Psychiatry 2007;61:880–9.
Cromwell HC, Mears RP, Wan L, Boutros NN. Sensory gating: a translational effort from basic to clinical science. Clin EEG Neurosci 2008;39:1–4.
Davis M, Heninger GR. Comparison of response plasticity between the eye-blink and the vertex potential in humans. Electroencephalogr Clin Neurophysiol 1972;33:283–93.

Eickhoff SB, Laird AR, Grefkes C, Wang LE, Zilles K, Fox PT. Coordinate-based activation likelihood estimation meta-analysis of neuroimaging data: a random-effects approach based on empirical estimates of spatial uncertainty. Hum Brain Map 2009;30:2907–26.
Eickhoff SB, Jbabdi S, Caspers S, Laird AR, Fox PT, Zilles K, et al. Anatomical and functional connectivity of cytoarchitectonic areas within the human parietal operculum. J Neurosci 2010;30:6409–21.
Eickhoff SB, Bzdok D, Laird AR, Roski C, Caspers S, Zilles K, et al. Co-activation patterns distinguish cortical modules, their connectivity and functional differentiation. Neuroimage 2011;57:938–49.
Eisenstein EM, Eisenstein D. A behavioral homeostasis theory of habituation and sensitization; further developments and predictions. Rev Neurosci 2006;17:533–57.
Franks R, Adler L, Waldo M, Alpert J, Freedman R. Neurophysiological studies of sensory gating in mania: comparison with schizophrenia. Biol Psychiatry 1983;18:989–1005.
Fuerst DR, Gallinat J, Boutros NN. Range of sensory gating values and test-retest reliability in normal subjects. Psychophysiology 2007;44:620–6.
Garcia-Rill E, Moran K, Garcia J, Findley WM, Walton K, Strotman B, et al. Magnetic sources of the M50 response are localized to frontal cortex. Clin Neurophysiol 2008;119:388–98.
Gjini K, Arfken C, Boutros NN. Relationships between sensory ''gating out'' and sensory ''gating in'' of auditory evoked potentials in schizophrenia: preliminary results. Schizophr Res 2010;121:139–45.
Gjini K, Burroughs S, Boutros NN. Relevance of attention in auditory sensory gating paradigms in schizophrenia: a pilot study. J Psychophysiol 2011;25:60–6.
Grau C, Fuentemilla LI, Marco-Pallarés. Functional neural dynamics underlying event-related N1 and N1 suppression response. Neuroimage 2007;36:522–31.
Grunwald T, Boutros NN, Pezer N, von Oertzen T, Fernandez G, Schaller C, et al. Neural substrates of sensory gating within the human brain. Biol Psychiatry 2003;53:511–9.
Guterman Y, Josiassen RC, Bashore Jr TR. Attentional influence on the P50 component of the auditory event-related brain potential. Int J Psychophysiol 1992;12:197–209.
Hanlon FM, Miller GA, Thoma RJ, Irwin J, Jones A, Moses SM. Distinct M50 and M100 auditory gating deficits in schizophrenia. Psychophysiology 2005;42:417–27.
Jääskeläinen IP, Ahveninen J, Bonmassar G, Dale AM, Ilmoniemi RJ, Levänen S, et al. Human posterior auditory cortex gates novel sounds to consciousness. PNAS 2004;101:6809–14.
Jerger K, Biggins C, Fein G. P50 suppression is not affected by attentional manipulations. Biol Psychiatry 1992;31:365–77.
Korzyukov O, Pflieger ME, Wagner M, Bowyer SM, Rosburg T, Boutros NN, et al. Generators of the intracranial P50 response in auditory sensory gating. Neuroimage 2007;35:814–26.
Korzyukov O, Asano E, Gumenyuk V, Juhász C, Wagner M, Rothermel RD, et al. Intracranial recording and source localization of auditory brain responses elicited at the 50 ms latency in three children aged from 3 to 16 years. Brain Topogr 2009;22:166–75.
Kral T, Clusmann H, Urbach J, Schramm J, Elger CE, Kurthen M, et al. Preoperative evaluation for epilepsy surgery (Bonn Algorithm). Zbl Neurochir 2002;63:106–10.
Krause M, Hofffmann WE, Hajos M. Auditory sensory gating in hippocampus and reticulalr thalamic neurons in anesthetized rats. Biol Psychiatry 2003;53:244–53.
Freedman R, Adler LE, Myles-Worsley M, Nagamoto HT, Miller C, Kisley M, et al. Inhibitory gating of an evoked response to repeated auditory stimuli in schizophrenia and normal subjects. Human recordings, computer simulation, and an animal model. Arch Gen Psychiatry 1996;53:1114–21.
Fuchs M, Wagner M, Kastner J. Development of volume conductor and source models to localize epileptic foci. J Clin Neurophysiol 2007;24:101–19.
Laird AR, Eickhoff SB, Li K, Robin DA, Glahn DC, Fox PT. Investigating the functional heterogeneity of the default mode network using coordinate-based meta-analytic modeling. J Neurosci 2009a;29:14496–505.
Laird AR, Eickhoff SB, Kurth F, Fox PM, Uecker AM, Turner JA. ALE meta-analysis workflows via the brainmap database: progress towards a probabilistic functional brain atlas. Front Neuroinformatics 2009b;3:23.
Liégeois-Chauvel C, Musolino A, Badier JM, Marquis P, Chauvel P. Evoked potentials recorded from the auditory cortex in man: evaluation and topography of the middle latency components. Electroencephalogr Clin Neurophysiol 1994;92:204–14.
Moxon KA, Gerhardt GA, Gulinello M, Adler LE. Inhibitory control of sensory gating in a computer model of the CA3 region of the hippocampus. Biol Cybern 2003;88:247–64.
Patterson JV, Hetrick WP, Boutros NN, Jin Y, Potkin S, Sandman C, et al. P50 sensory gating ratios in schizophrenics and controls: a review and data analysis. Psychiatry Res 2008;158:226–47.
Pascual-Marqui RD, Michel CM, Lehmann D. Low resolution electromagnetic tomography: a new method for localizing electrical activity in the brain. Int J Psychophysiol 1994;18:49–65.
Rentzsch J, Jockers-Scherübl MC, Boutros NN, Gallinat J. Test-retest reliability of P50, N100 and P200 auditory SG in healthy subjects. Int J Psychophysiol 2008;67:81–90.
Roemer R, Shagass C, Teyler TJ. Do human evoked potentials habituate? In: Peeke HVS, Petrinovich L, editors. Habituation, sensitization and behavior. Maryland Heights, MO: Academic Press; 1984. p. 325–46.
Rosburg T, Trautner P, Ludowig E, Helmstaedter C, Bien CG, Boutros NN. Sensory gating in epilepsy-effects of lateralization of hippocampal sclerosis. Clin Neurophysiol 2008;119:1310–9.
Sable JJ, Low KA, Maclin EL, Fabiani M, Gratton G. Latent inhibition mediates N1 attenuation to repeating sounds. Psychophysiology 2004;41:636–42.
Shan JC, Hsieh MH, Liu CM, Chiu MJ, Jaw FS, Hwu HG. More evidence to support the role of S2 in P50 studies. Schizophr Res 2010;122:270–2.
Siegel C, Waldo M, Mizner G, Adler LE, Freedman R. Deficits in sensory gating in schizophrenic patients and their relatives. Evidence obtained with auditory evoked responses. Arch Gen Psychiatry 1984;41:607–12.
Smith D, Boutros N, Schwarzkopf S. Reliability of P50 auditory event-related potential indices of sensory gating. Psychophysiology 1994;31:495–502.
Spencer SS, Sperling MR, Shewmon DA. Intracranial electrodes. In: Engel J, Pedley TA, editors. Epilepsy: a comprehensive textbook. New York: Lippincott-Raven; 1997. p. 607–12.
Stains WR, Black SE, Graham SJ, Mccllroy WE. Somatosensory gating and recovery from stroke involving the thalamus. Stroke 2002;33:2642–51.
Weiland BJ, Boutros NN, Moran JM, Tepley N, Bowyer SM. Evidence for a frontal cortex role in mediating both auditory and somatosensory habituation: a MEG study. NeuroImage 2008;42:827–35.
Weisser R, Weisbrod M, Roehrig M, Rupp A, Schroeder J, Scherg M. Is frontal lobe involved in the generation of auditory P50? Neuroreport 2001;12:3303–7.
Zouridakis G, Boutros NN. Stimulus parameter effects on the P50 evoked response (Brief Report). Biol Psychiatry 1992;32:839–41.
Venables P. Input dysfunction in schizophrenia. In: Maher BA, editor. Progress in experimental personality research. Orlando, FL: Academic Press; 1964. p. 1–47.